

A New Mixed Valent Molybdenum Monophosphate with a Tunnel Structure: $\text{Li}_x\text{Mo}_2\text{O}_3(\text{PO}_4)_2$

S. Ledain, A. Leclaire, M. M. Borel, and B. Raveau

Laboratoire CRISMAT-URA 1318, CNRS-ISMRA et Université de Caen, Boulevard du Maréchal Juin, 14050, Caen Cedex, France

Received July 31, 1995; in revised form October 20, 1995; accepted October 25, 1995

A new mixed valent molybdenum monophosphate, $\text{Li}_x\text{Mo}_2\text{O}_3(\text{PO}_4)_2$ with a tunnel structure has been synthesized. Although closely related to the monophosphate $\text{Na}_x(\text{Mo}, \text{W})_2\text{O}_3(\text{PO}_4)_2$, this phase differs from the latter by its triclinic symmetry with $a = 7.355(2)$ Å, $b = 6.361(2)$ Å, $c = 8.979(1)$ Å, $\alpha = 90.17(2)^\circ$, $\beta = 106.47(2)^\circ$, $\gamma = 90.26(2)^\circ$. The $[\text{Mo}_2\text{P}_2\text{O}_{11}]_\infty$ framework is very similar to that observed for the sodium phase: it consists of $\text{Mo}_2\text{PO}_{13}$ units linked to each other through single PO_4 tetrahedra forming infinite $[\text{Mo}_2\text{P}_2\text{O}_{15}]_\infty$ chains running along c . The main difference with respect to the monophosphate $\text{Na}_x(\text{Mo}, \text{W})_2\text{O}_3(\text{PO}_4)_2$ deals with the distribution of the Li^+ cations that are located in small tunnels with an octahedral coordination, whereas Na^+ ions are located in large tunnels with two kinds of coordination. This phase also differs from the molybdenotungsten monophosphate by the much lower amount of Mo(V). The distribution of the Mo(V) and Mo(VI) species over the two octahedral sites of the structure is discussed. © 1996

Academic Press, Inc.

INTRODUCTION

Started in 1990, the research on mixed valent molybdenum phosphates has allowed five series of Mo(V)–Mo(VI) monophosphate with an original structure in which the interpolated cation is a univalent element to be isolated (1–9). Among these numerous phosphates, only one, containing lithium, $\text{LiMo}_3\text{O}_4(\text{PO}_4)_3$ (9), has been synthesized to date. For this reason a systematic investigation of the Li–Mo–P–O system has been carried out. This investigation has also been encouraged by the recent discovery of a new monophosphate $\text{Na}_x(\text{Mo}, \text{W})_2\text{O}_3(\text{PO}_4)_2$, with an original tunnel structure (10), but which requires the presence of a large amount of tungsten for its stabilization. We report herein on a new molybdenum monophosphate $\text{Li}_x\text{Mo}_2\text{O}_3(\text{PO}_4)_2$ with a $[\text{Mo}_2\text{P}_2\text{O}_{11}]_\infty$ framework similar to that of the sodium phase $\text{Na}_x(\text{Mo}, \text{W})_2\text{O}_3(\text{PO}_4)_2$, but characterized by a different Mo(V)/Mo(VI) ratio and especially by a different occupancy of the tunnels of the structure.

EXPERIMENTAL

Single crystals of this new phosphate were grown from a mixture of nominal composition $\text{Li}_3\text{Mo}_{12}\text{P}_{11}\text{O}_{62}$. The synthesis was performed in two steps, using adequate ratios of MoO_3 , Mo, $\text{H}(\text{NH}_4)_2\text{PO}_4$, and Li_2CO_3 to obtain the above formulation. First, a mixture of MoO_3 , $\text{H}(\text{NH}_4)_2\text{PO}_4$, and Li_2CO_3 was ground and heated in air to 673 K to eliminate CO_2 , NH_3 , and H_2O . In a second step, the appropriate amount of molybdenum was added and the ground mixture was sealed in an evacuated silica ampoule, then heated for 1 day at 873 K, cooled at 4.5 K per hour to 773 K and finally quenched to room temperature. In the resulting mixture, the major phase occurred as black needles with a minor phase as a brown powder which was not identified. The microprobe analysis of the black needles leads to a Mo/P ratio (1/1) in agreement with the formula $\text{Li}_{0.21}\text{Mo}_2\text{P}_2\text{O}_{11}$ deduced from the structure determination. All the attempts to obtain pure powder failed; the X-ray patterns show only the MoPO_5 phase (11).

A black needle with dimensions $0.026 \times 0.141 \times 0.026$ mm³ was selected for the structure determination. The cell parameters were determined by diffractometric techniques at 294 K with a least-squares refinement based upon 25 reflections with $18^\circ < \theta < 22^\circ$. The data were collected with an Enraf–Nonius CAD4 diffractometer with the parameters reported in Table 1. The reflections were corrected for Lorentz and polarization effects and for absorption. The structure was solved with the heavy atom method. The refinements of the atomic parameters and the anisotropic thermal factors for Mo, P, and O atoms were successful in the space group $P\bar{1}$. Subsequent Fourier synthesis allowed the Li atoms to be localized. The refinement of the occupation of the Li atoms and its isotropic thermal factor led to the formulation $\text{Li}_{0.21}\text{Mo}_2\text{P}_2\text{O}_{11}$ with $R = 0.037$ and $R_w = 0.034$.

RESULTS AND DISCUSSION

Although similar to $\text{Na}_x(\text{Mo}, \text{W})_2\text{O}_3(\text{PO}_4)_2$, the lithium phosphate $\text{Li}_x\text{Mo}_2\text{O}_3(\text{PO}_4)_2$ exhibits a different symmetry.

TABLE 1
Summary of Crystal Data, Intensity Measurements,
and Structure Refinement Parameters for
 $\text{Li}_{0.21}\text{Mo}_2\text{P}_2\text{O}_{11}$

	1. Crystal data	
Space group	$P1$	
Cell dimensions	$a = 7.355(2) \text{ \AA}$	$\alpha = 90.17(2)^\circ$
	$b = 6.361(2) \text{ \AA}$	$\beta = 106.47(2)^\circ$
	$c = 8.979(1) \text{ \AA}$	$\gamma = 90.26(2)^\circ$
Volume (\AA^3)	$402.9(2) \text{ \AA}^3$	
Z	2	
ρ_{calc} (g cm^{-3})	3.56	
	2. Intensity measurements	
$\lambda(\text{MoK}\alpha)$	0.71073	
scan mode	ω -3/2 θ	
scan width ($^\circ$)	$1.1 + 0.35 \tan \theta$	
slit aperture (mm)	$1.1 + \tan \theta$	
max θ ($^\circ$)	45	
standard reflections	3 measured every 3600 sec	
measured reflections	6896	
reflections with $I > 3\sigma$	1992	
μ (mm^{-1})	3.49	
	3. Structure solution and refinement	
Parameters refined	138	
Agreement factors	$R = 0.037$ $R_w = 0.034$	
Weighting scheme	$w = 1/\sigma$	
Δ/σ max	<0.005	

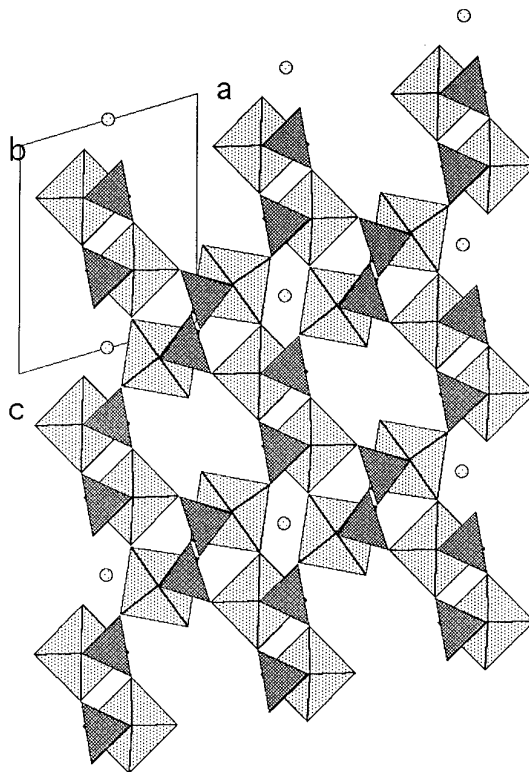


FIG. 1. Projection along b of the structure of $\text{Li}_{0.21}\text{Mo}_2\text{O}_3(\text{PO}_4)_2$ showing the $[\text{Mo}_2\text{P}_2\text{O}_{11}]_n$ framework with two types of tunnels.

It crystallizes in the triclinic system with $a = 7.355(2) \text{ \AA}$, $b = 6.361(2) \text{ \AA}$, $c = 8.979(1) \text{ \AA}$, $\alpha = 90.17(2)^\circ$, $\beta = 106.47(2)^\circ$, and $\gamma = 90.26(2)^\circ$, whereas the sodium phase is monoclinic with $a = 7.200(1) \text{ \AA}$, $b = 6.369(1) \text{ \AA}$, $c = 9.123(1) \text{ \AA}$, and $\beta = 106.29^\circ$. The atomic coordinates (Table 2) and the projection of the structure of $\text{Li}_x\text{Mo}_2\text{O}_3(\text{PO}_4)_2$ on to the (010) plane (Fig. 1) show that the $[\text{Mo}_2\text{P}_2\text{O}_{11}]_n$ framework is very similar to that previously observed for $\text{Na}_x(\text{Mo}, \text{W})_2\text{O}_3(\text{PO}_4)_2$ [10]. It consists of molybdenum bi-octahedra each sharing one apex with the same PO_4 tetrahedron P(2), forming $\text{Mo}_2\text{PO}_{13}$ units. Along c , the $\text{Mo}_2\text{PO}_{13}$ units are linked through single P(1) tetrahedra, forming infinite $[\text{Mo}_2\text{P}_2\text{O}_{15}]_n$ chains (Fig. 2). Note that this framework can also be described as the assemblage of $[\text{MoPO}_8]_n$ chains running along b , in which one MoO_6 octahedron alternates with one PO_4 tetrahedron (Fig. 3).

The geometry of the polyhedra that form the $[\text{Mo}_2\text{P}_2\text{O}_{11}]_n$ framework is very similar to that observed for the $[\text{Mo}_{1.17}\text{W}_{0.83}\text{P}_2\text{O}_{11}]_n$ host lattice of the sodium phosphate, as shown from the interatomic distances (Table 3). The PO_4 tetrahedra are very regular with P–O distances ranging from 1.51 to 1.55 \AA , in agreement with the fact that each of them shares its four apices with four MoO_6 octahedra. The Mo(1) octahedra exhibit two short Mo–O bonds (1.68–1.74 \AA), two intermediate ones (1.97–2.00 \AA) and two larger ones (2.13–2.15 \AA) very similar to those observed for the sodium molybdenotungstate, which is char-

TABLE 2
Positional Parameters and Their Estimated
Standard Deviations

Atom	x	y	z	B (\AA^2)	occupancy
Mo(1)	0.39393(8)	0.24913(9)	0.29487(6)	0.624(2)	1.
Mo(2)	0.16752(8)	0.25015(9)	0.84807(7)	0.656(2)	1.
P(1)	0.5117(2)	0.2481(3)	0.6751(2)	0.59(4)	1.
P(2)	0.9191(2)	0.2503(3)	0.1124(2)	0.61(4)	1.
Li	0.5	0.	0.	1.0(8) ^a	0.42(6)
O(1)	0.3672(6)	0.2464(7)	0.0959(5)	1.00(8)	1.
O(2)	0.6312(7)	0.2371(9)	0.3676(6)	1.8(2)	1.
O(3)	0.3540(6)	−0.0610(7)	0.3082(5)	0.96(8)	1.
O(4)	0.3616(6)	0.5550(7)	0.3090(5)	0.96(8)	1.
O(5)	0.0914(6)	0.2414(8)	0.2528(5)	1.04(8)	1.
O(6)	0.3580(6)	0.2457(7)	0.5225(5)	0.88(8)	1.
O(7)	0.0340(7)	0.232(1)	0.6665(6)	2.24(2)	1.
O(8)	0.2102(6)	−0.0573(7)	0.8922(6)	1.04(8)	1.
O(9)	0.2046(7)	0.5554(7)	0.8804(6)	1.12(2)	1.
O(10)	0.9750(6)	0.2578(7)	0.9593(5)	1.04(8)	1.
O(11)	0.4226(6)	0.2426(8)	0.8107(5)	1.04(8)	1.

Note. Anisotropically refined atoms are given in the form of the isotropic equivalent displacement parameter defined as: $B = 4/3 \sum_i \sum_j \mathbf{a}_i \cdot \mathbf{a}_j \cdot \beta_{ij}$.

^a Atom isotropically refined.

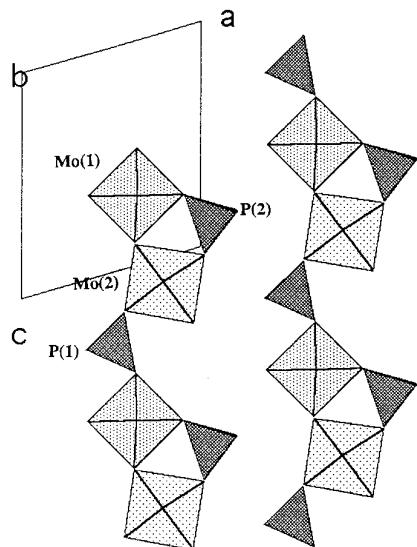


FIG. 2. The $[\text{Mo}_2\text{P}_2\text{O}_{15}]_\infty$ chains along c built up from $\text{Mo}_2\text{PO}_{13}$ units.

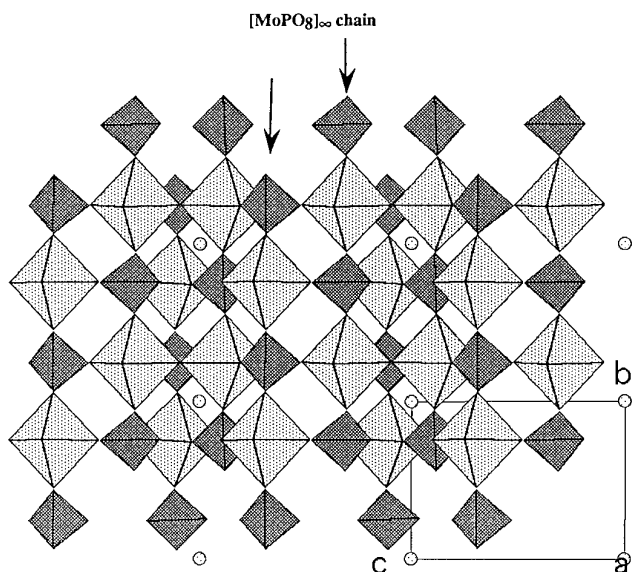


FIG. 3. The $[\text{MoPO}_8]_\infty$ chains along b .

TABLE 3
Distances (Å) and Angles (°) in the Polyhedra

Mo(1)	O(1)	O(2)	O(3)	O(4)	O(5)	O(6)
O(1)	1.742(5)	2.654(6)	2.756(7)	2.747(7)	2.779(7)	3.850(7)
O(2)	101.6(2)	1.683(5)	2.717(7)	2.784(7)	3.808(7)	2.749(7)
O(3)	94.5(2)	94.6(2)	2.002(5)	3.919(7)	2.678(7)	2.730(7)
O(4)	95.3(2)	99.0(2)	161.3(2)	1.970(5)	2.752(7)	2.756(6)
O(5)	90.5(2)	167.2(2)	80.3(2)	83.7(2)	2.149(5)	2.648(6)
O(6)	166.9(2)	91.4(2)	82.5(2)	84.3(2)	76.4(2)	2.134(5)
Mo(2)	O(7)	O(8)	O(9)	O(10) ⁱ	O(11)	O(1) ⁱⁱ
O(7)	1.651(5)	2.779(7)	2.845(7)	2.788(8)	2.784(6)	3.939(6)
O(8)	98.5(3)	2.005(5)	3.899(6)	2.826(7)	2.691(7)	2.677(6)
O(9)	103.2(3)	157.8(2)	1.969(5)	2.756(7)	2.741(7)	2.788(6)
O(10) ⁱ	101.1(2)	91.2(2)	89.3(2)	1.951(5)	3.888(7)	2.797(6)
O(11)	99.0(2)	84.5(2)	87.4(2)	159.9(2)	1.998(5)	2.704(7)
O(1) ⁱⁱ	174.4(3)	76.8(2)	81.3(2)	82.1(2)	77.8(2)	2.292(4)
P(1)	O(3) ⁱⁱⁱ	O(4) ^{iv}	O(6)	O(11)		
O(3) ⁱⁱⁱ	1.531(5)	2.444(7)	2.527(7)	2.487(7)		
O(4) ^{iv}	105.5(3)	1.540(5)	2.519(7)	2.508(7)		
O(6)	112.5(3)	111.4(3)	1.509(4)	2.496(6)		
O(11)	108.2(3)	109.2(3)	110.0(3)	1.538(6)		
P(2)	O(5) ^{vi}	O(8) ⁱⁱⁱ	O(9) ^{iv}	O(10) ^v		
O(5) ^{vi}	1.515(4)	2.514(6)	2.530(6)	2.532(6)		
O(8) ⁱⁱⁱ	110.6(3)	1.543(5)	2.465(7)	2.507(7)		
O(9) ^{iv}	111.2(3)	105.7(3)	1.550(5)	2.513(7)		
O(10) ^v	111.8(3)	108.6(3)	108.6(3)	1.543(5)		

Note. The Mo–O or P–O distances are on the diagonal, above it are the $\text{O} \cdots \text{O}$ distances, and below it are the O–Mo–O or O–P–O angles.

Symmetry codes: (i) $x - 1, y, z$; (ii) $x, y, z + 1$; (iii) $1 - x, y, 1 - z$; (iv) $1 - x, 1 - y, 1 - z$; (v) $x, y, z - 1$; (vi) $x + 1, y, z$. Li–O(1), 2.153(5) Å; Li–O(8)^v, 2.106(4) Å; Li–O(11)^v, 2.252(5) Å; Li–O(1)^{vi}, 2.153(5) Å; Li–O(8)^{vi}, 2.106(4) Å; Li–O(11)^{vi}, 2.252(5) Å.

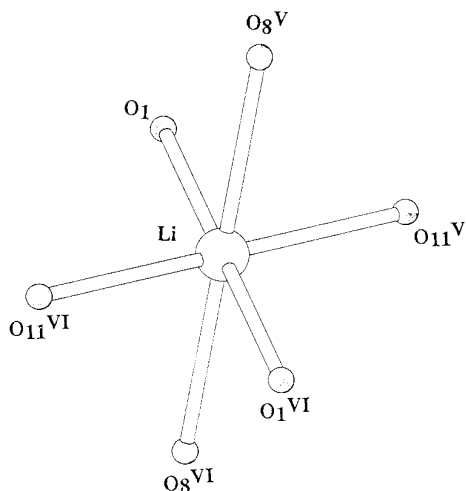


FIG. 4. Octahedral coordination of the lithium.

acterized by pairs of (Mo–W)–O bonds of 1.71–1.73, 1.977–1.977, and 2.14–2.15 Å, respectively. In a similar way the Mo(2) octahedra exhibit one shorter Mo–O bond of 1.65 Å, four intermediate Mo–O bonds ranging from 1.95 to 2.00 Å, and a larger one of 2.29 Å, to be compared to 1.69 Å, 1.96–1.98 Å, and 2.21 Å, respectively for $\text{Na}_x(\text{Mo}, \text{W})_2\text{O}_3(\text{PO}_4)_2$. It is worth pointing out that both Mo(1) and Mo(2) octahedra exhibit one free oxygen apex, which is currently observed in Mo(V) compounds. Nevertheless the geometry of the Mo(1) octahedra suggests that the site is fully occupied by Mo(VI) whereas Mo(V) should be localized on Mo(2), according to the formulation $\text{Li}_{0.21}(\text{Mo}^{\text{VI}})_{\text{M1}}(\text{Mo}_{0.78}^{\text{VI}}\text{Mo}_{0.21}^{\text{V}})_{\text{M2}}\text{O}_3(\text{PO}_4)_2$, in agreement with the formula previously proposed for the sodium molybdenotungstenphosphate $\text{Na}_{0.75}(\text{Mo}_{0.42}^{\text{VI}}\text{W}_{0.58}^{\text{VI}})_{\text{M1}}(\text{Mo}_{0.75}^{\text{V}}\text{W}_{0.25}^{\text{VI}})_{\text{M2}}\text{O}_3(\text{PO}_4)_2$. This distribution of the Mo(V) and Mo(VI) species is also supported by the valence calculations using the Brown and Altermatt expression (12): one indeed obtains a valence of 6.04 for Mo(1) and 5.64 for Mo(2).

The important difference between the two structures deals with the distribution of the interpolated cations in the tunnels of the structure. One indeed observes that the large tunnels are empty in the lithium molybdenophosphate

whereas they are occupied by sodium with two kinds of coordination in the molybdenotungsten phosphate. In fact, the Li^+ cations are located in smaller tunnels of the structure (Fig. 1) that were empty in the sodium molybdenotungsten phosphate. In these tunnels, lithium exhibits an octahedral coordination (Fig. 4) with Li–O distances ranging from 2.106 to 2.252 Å.

Another difference due to the triclinic distortion is that one observes in the Li compound a little waving toward **b** of the chains running along **c**, whereas in the Na compound, the centers of the polyhedra all lie in the same plane.

These results show the great ability of this $[\text{Mo}_2\text{P}_2\text{O}_{11}]_\infty$ framework to accommodate cations with various coordinations and size. They suggest the possible existence of non-stoichiometric monophosphates $\text{Li}_x\text{Na}_y\text{Mo}_2\text{O}_3(\text{PO}_4)_2$, characterized by a simultaneous occupation of the two kinds of tunnels by lithium and sodium, respectively. An investigation of the system Li–Na–Mo–P–O will be performed.

REFERENCES

1. G. Costentin, M. M. Borel, A. Grandin, A. Leclaire, and B. Raveau, *J. Solid State Chem.* **95**, 168 (1991).
2. A. Guesdon, M. M. Borel, A. Grandin, A. Leclaire, and B. Raveau, *C.R. Acad. Sci.* **316**, 477 (1993).
3. A. Guesdon, M. M. Borel, A. Grandin, A. Leclaire, and B. Raveau, *J. Solid State Chem.* **109**, 145 (1994).
4. M. M. Borel, A. Leclaire, A. Grandin, and B. Raveau, *J. Solid State Chem.* **108**, 336 (1994).
5. M. M. Borel, A. Guesdon, A. Leclaire, A. Grandin, and B. Raveau, *Z. Anorg. Allg. Chem.* **108**, 336 (1994).
6. M. M. Borel, A. Leclaire, A. Guesdon, A. Grandin, and B. Raveau, *J. Solid State Chem.* **112**, 150 (1994).
7. T. Hoareau, A. Leclaire, M. M. Borel, A. Grandin, and B. Raveau, *J. Solid State Inorg. Chem.* **31**, 727 (1994).
8. T. Hoareau, A. Leclaire, M. M. Borel, A. Grandin, and B. Raveau, *J. Solid State Chem.* **116**, 87 (1995).
9. T. Hoareau, M. M. Borel, A. Leclaire, J. Provost, and B. Raveau, *Mater. Res. Bull.* **30**, 523 (1995).
10. A. Leclaire, M. M. Borel, J. Chardon, and B. Raveau, *J. Solid State Chem.* **120**, 353 (1995).
11. P. Kierkegaard and M. Westerlund, *Acta Chem. Scand.* **18**, 2217 (1964).
12. L. D. Brown and D. Altermatt, *Acta Crystallogr. Sect. B* **41**, 244 (1985).